Smooth Path Planning for a Biologically-Inspired Neurosurgical Probe

Sophia Bano[1], Seong Young Ko[2], *Member, IEEE*, Ferdinando Rodriguez y Baena[3], *Member, IEEE*

Abstract— Percutaneous intervention involves the insertion of needles to specific locations inside the human body, to perform a variety of surgical procedures. Percutaneous procedures are becoming the preferred choice for many neurosurgeons, due to the additional benefits they provide over conventional open neurosurgery. A neurosurgical flexible and steerable probe named STING is currently being developed for accessing deep brain lesions following curvilinear paths. In this paper, we present a path planning method for generating pre-operative paths for this neurosurgical flexible probe. Since the flexible probe is modeled as a nonholonomic system, a deterministic continuous curvature path planning scheme capable of avoiding obstacles is developed for smooth steering of its tip. Multiple paths are generated by varying arrival angle at the targeted lesion and a path optimization approach is then formulated, with the aim to minimize damage to the tissue (i.e. shortest path) and the risk to the patient (obstacle avoidance). Simulation results are reported using the risk-map generated for a coronal slice of the brain, which confirms the successful design of a path planning scheme that satisfies the nonholonomic constraints of the neurosurgical probe.

I. INTRODUCTION

With the recent advances in medical imaging modalities, percutaneous interventions are becoming the preferred choice in neurosurgical procedures, since they provide benefits of reduced trauma, less pain and short recovery time to the patient. These interventions require insertion of probes, needles or electrodes inside the brain, using CT or MRI images, to precisely target lesions, while avoiding obstacles such as sensitive tissue, nerves or arteries.

Thick and non-flexible needles are easily pointed to the target but their manipulation causes significant pressure on the tissue. Moreover, straight needles are not suitable for following curved paths, if obstacle avoidance is required. These problems can be solved by using thin and flexible needles. Thus, a biologically-inspired neurosurgical flexible and steerable probe named STING (Soft-Tissue Intervention and Neurosurgical Guide) [1] is currently being developed at Imperial College London, with the aim to access deep brain lesions, while ensuring minimum damage to the patient. The flexible probe is currently capable of steering in two

[1]S. Bano was at Imperial College and is now a PhD student of the EMJD ICE at Queen Mary, University of London, UK sophia.bano@eecs.qmul.ac.uk

[2]S. Y. Ko was at Imperial College and is now with the School of Mechanical Systems Engineering, Chonnam National University, Gwangju, South Korea sko@chonnam.ac.kr

[3]F. Rodriguez y Baena is with the Mechanical Engineering Dept., Imperial College, London, UK (corresponding author) f.rodriguez@imperial.ac.uk

dimensional space and is modeled as a nonholonomic system [2]. Mechanical constraints of this probe impose a minimum radius of curvature constraint on the path. Furthermore, the probe kinematics require the curvature to be continuous.

Recently, Alteroviz *et al.* [3] resolved the motion planning problem for a special class of flexible bevel-tip needle, resulting in a trajectory that avoids obstacles while accounting for needle motion uncertainties. This technique, however, cannot be used for our flexible probe due to its mechanical constraints [1]. There is a need for a pre-operative path planning method for the flexible probe, which should mainly satisfy its curvature continuity constraint.

Several methods already exist for the path planning of mobile robots, which can be applied to the flexible probe. A prevalent method in the literature uses Dubins curves, which uses line segments and circular arcs to generate the shortest path having discontinuous curvature [4][5]. Variants of Dubins curves make use of the clothoid pairs along with line segments and circular arcs, resulting in continuous curvature paths [6]. However, such curves do not have a closed-form expression of the position [5]. Moreover, they are not flexible in matching the endpoint conditions of the path and are not suitable in the presence of obstacles [7].

Path planning is also addressed using probabilistic methods, where an iterative approach is used to achieve a near optimum solution. Examples of these include Probablistic Road Maps (PRMs) [8] and Rapidly-exploring Random Trees (RRTs) [9]. Patil and Alterovitz [10] demonstrated a motion planning method using reachability guided rapidly exploring random trees (RG-RRT). Recently, Alterovitz *et al.* [11] also presented a rapidly-exploring road-map based approach for path planning. However, these approaches do not guarantee an optimum solution and are unable to generate curvature continuous paths without further modification.

Nagy and Kelly [12] and Thompson and Kagami [13] proposed a deterministic approach for the optimization of curvature to obtain continuous and smooth paths for nonholonomic robots. This method generates continuous curvature paths by modeling the curvature as a polynomial. Thus, we adopt a similar approach for the path planning of the neurosurgical flexible probe.

In this paper, a gradient method is proposed using [12] and [13] for the path planning of the flexible probe, since it provides the additional advantage of generating continuous curvature paths. Section II gives an introduction to STING. Section III details the mechanical constraints of STING and the proposed approach for solving the path planning problem. Simulation results are presented in Section IV. Conclusion and future work are detailed in Section V.
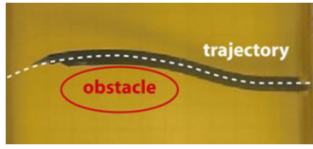
Fig. 1: Soft-Tissue Intervention and Neurosurgical Guide

II. STING: SOFT-TISSUE INTERVENTION AND NEUROSURGICAL GUIDE

The design of STING is inspired by the ovipositor of wood wasps, which is used to penetrate the bark of wood to deliver eggs [1]. It is designed to steer in brain-like tissue, while avoiding sensitive anatomical areas to reach a deep-seated target at minimum risk to the patient. Figure 1 shows the steering of STING in a gelatine sample of brain-like consistency, as in [1]. This flexible probe consists of four interlocked segments, which are capable of sliding independently with respect to each other. Control of the steering angle is achieved by varying the offset between segments, where the relationship between offset and curvature was found to be approximately linear [2].

The overall system architecture of the flexible probe is illustrated in Fig. 2. It consists of two main blocks: path planning and path following. This paper focuses on the former, which takes the pre-operative diagnostic images (Magnetic Resonance Images showing the location of the deep brain target) and the physical constraints imposed by the flexible probe as input, and provides a planned path with minimum risk as output. Preliminary results of a path following approach which was successful on a scaled-up 12mm probe prototype can be found in [2].

In this paper, we aim to compute the optimal path for the neurosurgical flexible probe from a given start point to a lesion identified on a 2D brain slice, while respecting the probe's mechanical constraints. We also implement a risk-based path planning approach, where the anatomical regions on a 2D coronal section of the brain have been labeled according to the level of risk experienced by the patient if it was to be traversed, from 'accessible' to 'avoid'.
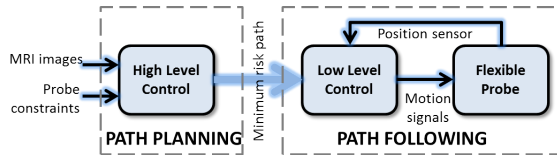

Fig. 2: System architecture of the flexible probe

III. CONTINUOUS CURVATURE PATH PLANNER

A. Mechanical Constraints of the Flexible Probe

The flexible probe is capable of changing its direction with the help of a 'programmable bevel-tip'. An off-line continuous path planner is needed due to the mechanical limitations of the probe. These limitations are as follows:

1) The maximum curvature should be bounded, resulting in a minimum radius of curvature constraint.

2) A drastic change in curvature is not allowed; hence the curvature should be continuous.

3) The rate of change of curvature should also be bounded in order to reduce damage to the tissue.

Gradient-based nonlinear optimization methods are useful for generating smooth paths for nonholonomic robots [14]. We modified this method to adapt it for the path planning of a flexible probe because it successfully generates a continuous curvature path while avoiding obstacles. The cost function for obstacle avoidance is designed to cater for irregular shaped obstacles and to guarantee fast processing. The bound on maximum curvature and its derivative is achieved by calculating multiple paths while varying the arrival angle at a target and selecting the one which satisfies these constraints.

B. The Approach

1) Path Planning without Obstacle Avoidance: Let $\underline{x}_0 = [x_0, y_0, \theta_0, \kappa_0]^T$ and $\underline{x}_T = [x_T, y_T, \theta_T, \kappa_T]^T$ be the start and target postures of the flexible probe. The gradient method optimizes the cubic curvature polynomial to generate deterministic continuous path between these postures. For a configuration space free of obstacles, the solution to the state equations is given in [12]:

$$
\begin{aligned}
x(s) &= x_0 + \int_0^s \cos(\theta(\tau))d\tau \ , \\
y(s) &= y_0 + \int_0^s \sin(\theta(\tau))d\tau \ , \\
\theta(s) &= \theta_0 + \int_0^s \kappa(\tau)d\tau \ , \\
\kappa(s) &= \kappa_0 + as + bs^2 + cs^3 \ ,
\end{aligned}
\tag{1}
$$

where (a, b, c) are the coefficients of the polynomial and s is the arc length. The parameter vector $\underline{p} = [a, b, c, s]^T$ is initialized and the path is computed by iteratively updating $\underline{p}$. The convergence of the algorithm is guaranteed only if the termination conditions are satisfied [12].

The set of non-linear equations in (1) can be re-written in vector form as $\underline{x} = \underline{f}(\underline{p})$, which can be linearized as follows:

$$
\Delta \underline{x} = [\frac{\partial}{\partial \underline{p}}\underline{f}]\Delta \underline{p} \ .
\tag{2}
$$

Since the degrees of freedom to control the entire endpoint state are available, its Jacobian has sufficient rank and is invertible. Thus, we solved it iteratively using (3), until convergence is achieved.

$$
\Delta \underline{p} = [\frac{\partial}{\partial \underline{p}}\underline{f}]^{-1}\Delta \underline{x} \ .
\tag{3}
$$

The problem is treated as an inverse kinematics computation. Starting with an initial guess of $\underline{p}$, the forward solution is calculated using (1) to get the end point $\hat{\underline{x}}$ for the proposed path. The Jacobian and difference $\Delta \underline{x} = \hat{\underline{x}} - \underline{x}_T$ are calculated and $\Delta \underline{p}$ is obtained using (3). Finally, the parameters update is computed using:

$$
\underline{p} = \underline{p} + \mu\Delta \underline{p} \ ,
\tag{4}
$$

where μ represents a constant gain. The process is repeated until $\underline{p}$ converges to an acceptable trajectory, while $\Delta \underline{x}$ tends towards zero [12]. The complete method is summarized in Algorithm 1.

921

Algorithm 1 $\underline{p} \leftarrow$ GRADIENT_METHOD$(\underline{x}_0, \underline{x}_T)$

1: $\underline{p} \leftarrow$ INITIALIZE_PARAMETER_VECTOR$(\underline{p})$
2: **while** $(\Delta \underline{x} \not\approx 0)$ **do**
3:     Compute forward solution $\underline{x}'$
4:     Compute Jacobian and $\Delta \underline{x}$
5:     Calculate $\Delta \underline{p}$ using eq. (3)
6:     Update parameter vector $\underline{p}$ using eq. (4)
7: **end while**

---

2) Path Planning with Obstacle Avoidance: The cubic curvature trajectories are extended to fourth-order polynomials and a cost function (L) is introduced, which describes the accumulated distance to obstacles along a trajectory [13]. The posture vector is now given by $\underline{x} = [x, y, \theta, \kappa, L]^T$. The trajectory generated using the fourth-order polynomial as curvature model satisfies the continuity constraints and avoids obstacles. A control point is added to parameters and the curvature polynomial is given by:

$$\kappa(s) = \kappa_0 + as + bs^2 + cs^3 + ds^4 . \quad (5)$$

The state parameters $\theta(s), x(s), y(s)$ are computed accordingly using (1). The new term L, describing the cost imposed by the presence of obstacles, is formulated as in [13]:

$$L(s) = \int_0^s (\frac{\lambda}{\nu_0} + \cdots + \frac{\lambda}{\nu_{N-1}})d\tau , \quad (6)$$

where λ describes the repulsive quality of obstacles and ν_i is the distance between a robot posture and an obstacle i.

A continuous curvature path is generated using a cubic polynomial, which is checked for obstacle collisions. If the resultant path collides with an obstacle, the approach is extended to a fourth-order polynomial optimization, where the parameter $\underline{p} = [a, b, c, d, s]$ is initialized using the result of the cubic curvature optimization and the cost function is calculated using (6). Algorithm 1 is then followed until convergence is achieved.

The cost function L, from [13], has several limitations. It does not take into account irregular-shaped obstacles. Furthermore, L becomes computationally expensive in the presence of many obstacles, thus reducing overall efficiency.

Unlike [13], we propose a new cost function L_{new} to overcome the above limitations. L_{new} is defined such that it only consider obstacles lying in the local neighbourhood of the trajectory during the iterative update of the algorithm. We use a local neighbourhood window of size $(2D_c + 1) \times (2D_c + 1)$ (where D_c is the clearance required from the obstacles). We slide this window over the initial trajectory generated by the cubic curvature polynomial and capture the trajectory information, which is then convolved with a 2D Gaussian kernel. Finally, we define a distance measure $D(s)$ using the above information, which is given by:

$$D(s)_j = D_c - D_c O(x_j, y_j) , \quad (7)$$

where x_j and y_j are the x and y coordinates of the jth sampled trajectory point and $O(x_j, y_j)$ is given by:
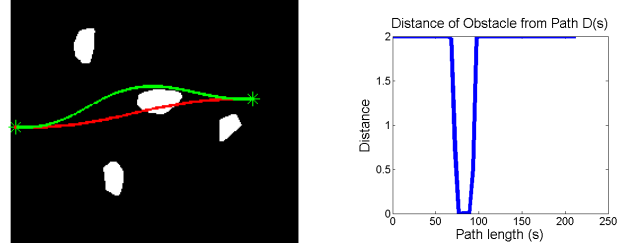
(a) A configuration space showing third (red) and fourth order (green) trajectories

(b) Distance D(s) for first instant of red trajectory

Fig. 3: Irregular shaped obstacles (white) are avoided using L_{new}, resulting in fourth order continuous curvature paths

$$O(x_j, y_j) = \sum_{k=-D_c}^{D_c} \sum_{l=-D_c}^{D_c} I(x_j + k, y_j + l) G(k, l) , \quad (8)$$

where I and G represent the configuration space and Gaussian kernel, respectively. Thus, the new cost function L_{new} is given by:

$$L_{new} = \int_0^s (\frac{\lambda}{D(\tilde{s})_j}) d\tilde{s} - s \frac{\lambda}{D_c} . \quad (9)$$

Figure 3 shows the result obtained in an example configuration space containing irregular shaped obstacles. Note that the value $O(x_j, y_j)$ will be high when the trajectory is occluded by obstacles, thus resulting in a low value of $D(s_j)$. Hence, this newly designed L_{new} produces an obstacle free path by deforming the trajectory of a cubic polynomial into a fourth order polynomial.

C. Path Optimization

We generate multiple paths by varying the target orientation θ, since this is required in order to implement risk-based path planning on a 2D risk-map of the brain. The continuous curvature paths satisfying the maximum curvature constraint are then selected as the most feasible paths. The optimal path is the one having the minimum value for the following cost function [15]:

$$C_i = \alpha \frac{\phi_i}{max(\phi)} + \beta \left(1 - \frac{\psi_i}{max(\psi)}\right) + \gamma \frac{\eta_i}{max(\eta)} \quad (10)$$

where C_i refers to the ith path's cost, ϕ_i is the length of the path, ψ_i is the minimum distance from an obstacle, and η_i is the accumulated risk along the path. The weighting parameters α, β, γ are defined by the user, such that $\alpha + \beta + \gamma = 1$.

IV. SIMULATION RESULTS

The algorithm was developed using MATLAB $v.7.9$, on an Intel Core 2 CPU 6300@1.86GHz processor. The flexible probe, with a thickness of $4mm$ (outer diameter), is constrained with a maximum curvature of 0.01 $(1/mm)$. The control error is arbitrarily set to $2mm$. The generated path should thus have a clearance of $4mm$ from any obstacles.
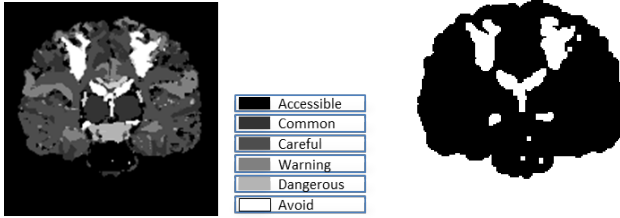
922

Fig. 4: Formation of configuration space (right) from the risk-map of a brain (left), with six levels of risk labeled
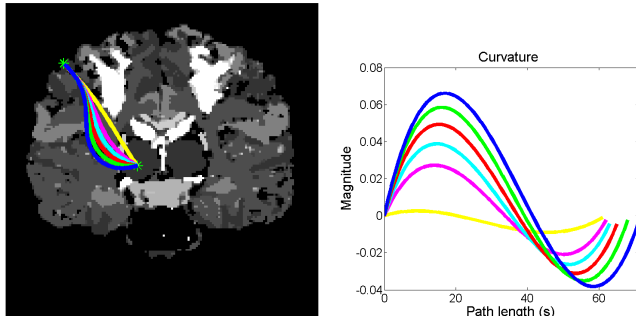

Fig. 5: Gradient based path planner showing the effect of varying target orientation θ (left) and curvature κ (right)
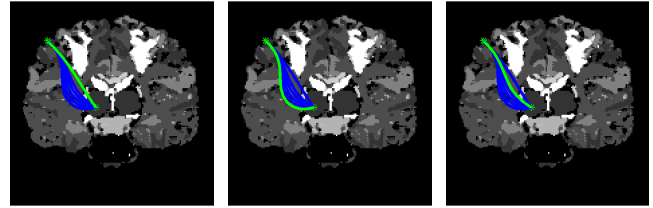

Fig. 6: Results for optimization of path showing (in green) the shortest path $(\alpha, \beta, \gamma) = (1, 0, 0)$ (left), path with maximum clearance from the obstacle $(\alpha, \beta, \gamma) = (0, 1, 0)$ (middle), path with minimum risk $(\alpha, \beta, \gamma) = (0, 0, 1)$ (right)

clearance from obstacles and minimum risk to the patient. Future work involves incorporation of soft tissue deformation during insertion to reduce placement error and extension of the path planner to 3D, since the neurosurgical flexible probe design will eventually allow it to steer in 3D space.

Simulations were performed on a 2D risk-map (153×153 pixels) generated from a coronal slice of the brain, using a scale of $1\ pixel = 1mm$. The main structure of the brain was arbitrarily classified into six 'risk-values', namely *Accessible, Common, Careful, Warning, Dangerous, Avoid*, as shown in Fig. 4. Each risk-value was then assigned a greyscale value ranging from 0 to 255, where black denotes an accessible and white denotes an impenetrable area. The configuration space is formed by considering the highest risk-value, i.e. 'AVOID' and dilating it by the thickness of the flexible probe.

The start pose $(60mm, 60mm, \pi/4)$ and target position $(130mm, 160mm)$ are selected as input for the algorithm. The start and target values of curvature (κ) are arbitrarily set to $0.008(1/mm)$, while a range of target orientations in the range $(-0.2\ to\ 1.0rad)$ were selected manually. By varying the target orientation θ_T, several continuous curvature paths were generated and the result is shown in Fig. 5. The optimal path is selected by using (10). The result for different values of weighting parameters α, β, γ are shown in Fig. 6.

V. CONCLUSIONS

A bespoke gradient-based method for the continuous and smooth path planning of steering probes has been developed by modifying existing approaches available in the literature. These changes were introduced to satisfy the specific mechanical constraints of a flexible probe inspired by the egg-laying channel of certain insects, by allowing both the curvature and the curvature derivative to be bounded and continuous. A path optimization scheme is also reported, which computes an optimum path based on predefined criteria, while ensuring minimum damage to the tissue, maximum

REFERENCES

[1] L. Frasson, S. Ko, A. Turner, T. Parittotokkaporn, J. Vincent, and F. Rodriguez y Baena, "Sting: a soft-tissue intervention and neurosurgical guide to access deep brain lesions through curved trajectories," *Proceedings of the Institution of Mechanical Engineers, Part H: Journal of Engineering in Medicine*, vol. 224, no. 6, p. 775, 2010.

[2] S. Ko, L. Frasson, and F. Rodriguez y Baena, "Closed-loop planar motion control of a steerable probe with a"programmable bevel"inspired by nature," *IEEE Transactions on Robotics*, no. 99, pp. 1–14, 2011.

[3] R. Alterovitz, M. Branicky, and K. Goldberg, "Motion planning under uncertainty for image-guided medical needle steering," *International journal of robotics research*, vol. 27, no. 11-12, pp. 1361–1374, 2008.

[4] J. Barraquand and J. Latombe, "On nonholonomic mobile robots and optimal maneuvering," in *IEEE International Symposium on Intelligent Control, 1989. Proceedings*, pp. 340–347, IEEE, 1989.

[5] O. Pinchard, A. Liegeois, and F. Pougnet, "Generalized polar polynomials for vehicle path generation with dynamic constraints," in *IEEE International Conference on Robotics and Automation*, vol. 1, pp. 915–920, IEEE, 1996.

[6] T. Fraichard and A. Scheuer, "From reeds and shepp's to continuous-curvature paths," *IEEE Transactions on Robotics*, vol. 20, no. 6, pp. 1025–1035, 2004.

[7] D. J. Walton, D. S. Meek, and J. M. Ali, "Planar g2 transition curves composed of cubic bezier spiral segments," *J. Comput. Appl. Math.*, vol. 157, pp. 453–476, August 2003.

[8] R. Geraerts and M. Overmars, "A comparative study of probabilistic roadmap planners," *Algorithmic Foundations of Robotics V*, 2004.

[9] S. LaValle and J. Kuffner Jr, "Rapidly-exploring random trees: Progress and prospects," 2000.

[10] S. Patil and R. Alterovitz, "Interactive motion planning for steerable needles in 3d environments with obstacles," in *Biomedical Robotics and Biomechatronics (BioRob), 2010 3rd IEEE RAS and EMBS International Conference on*, pp. 893–899, IEEE, 2010.

[11] R. Alterovitz, S. Patil, and A. Derbakova, "Rapidly-exploring roadmaps: Weighing exploration vs. refinement in optimal motion planning," in *IEEE International Conference on Robotics and Automation (ICRA)*, pp. 3706–3712, IEEE, 2011.

[12] B. Nagy and A. Kelly, "Trajectory generation for car-like robots using cubic curvature polynomials," *Field and Service Robots*, vol. 11, 2001.

[13] S. Thompson and S. Kagami, "Continuous curvature trajectory generation with obstacle avoidance for car-like robots," *International Conference on Computational Intelligence for Modelling, Control and Automation*, 2005.

[14] H. Choset, *Principles of robot motion: theory, algorithms, and implementation*. The MIT Press, 2005.

[15] C. Caborni, S. Ko, E. Momi, G. Ferrigno, and F. Rodriguez y Baena, "Optimization of rapidly-exploring random trees (rrt)-based path planning for a neurosurgical steerable probe," in *Proceedings of The Hamlyn Symposium on Medical Robotics,*, 2011.

923